Exciton-mediated Raman scattering in multiple quantum wells

Bangfen Zhu
Center of Theoretical Physics, Chinese Center for Advanced Science and Technology (World Laboratory), Beijing, China and Institute of Semiconductors, Chinese Academy of Sciences, P.O. Box 912, Beijing 100 083, China

Kun Huang and Hui Tang
Institute of Semiconductors, Chinese Academy of Sciences, P.O. Box 912, Beijing 100 083, China
(Received 15 May 1989)

The main results of a microscopic theory on the resonant Raman profile mediated by exciton states in multiple quantum wells (MQW's) are presented. The theory takes proper account of effects of heavy- and light-hole mixing of the exciton states, and adopts an appropriate expression for electron-phonon interaction. The selection rules on exciton–LO-phonon scattering in MQW's are summarized, which reveals the roles played by intrasubband and intersubband exciton Raman scattering. Numerical calculations show the dependence of exciton-phonon scattering on the well width and the phonon modes. The mechanism for the asymmetry of the incoming and outgoing resonance is discussed.

Owing to carrier confinement in the growth direction of quantum wells, discrete free-exciton states play a dominant role in optical processes in multiple quantum wells (MQW's). These exciton states, as intermediate states, should contribute importantly to the one-phonon Raman effect, as may be surmised from a number of experiments on the resonant Raman profile.[1–3] In the present paper, we shall report on the main results of a systematic theoretical treatment of the subject.

Previously, certain theoretical knowledge has been of basic importance in the interpretation of Raman scattering experiments carried out on MQW's such as polarization selection rules relating to phonon symmetry and the electron-phonon interaction mechanism. Also, it has been known that, unlike bulk materials, Fröhlich interaction is no longer dipole forbidden in MQW's. This is important in understanding why $A1$ modes were observed under nonresonant conditions.[4–6] However, a systematic microscopic theory is still lacking. As we shall show, a microscopic treatment, especially one which incorporates the recent advances in our understanding of electron structure,[7–9] exciton states,[10–12] and phonon modes,[13–16] will be basic to a proper understanding of the subject. For the sake of simplicity, we shall work under the so-called cylindrical approximation (that is, if the growth direction of MQW's is taken to be the z axis, the electron and phonon Hamiltonian in the xy plane will be treated isotropically), and the dipole approximation (i.e., treating the photon wave numbers as vanishingly small). Furthermore, in this paper the only situation we consider is the backscattering $z\bar{z}$ configuration.

The Stokes-Raman tensor associated with the incident photon energy E and emitted phonon frequency ω_q is expressed as follows:[17]

$$\frac{1}{m_0}\sum_{\alpha,\beta}\frac{\langle 0|\mathbf{P}\cdot\hat{\boldsymbol{\varepsilon}}_s|\beta\rangle\langle\beta|H_{e\text{-}p}|\alpha\rangle\langle\alpha|\mathbf{P}\cdot\hat{\boldsymbol{\varepsilon}}_i|0\rangle}{(E_\alpha-E)(E_\beta+\hbar\omega_q-E)}\,, \tag{1}$$

where $\hat{\boldsymbol{\varepsilon}}_i$ and $\hat{\boldsymbol{\varepsilon}}_s$ are unit polarization vectors for incident and scattered light, respectively. $|\alpha\rangle$ and $|\beta\rangle$ denote the intermediate exciton states associated with energies E_α and E_β. The Hamiltonian for Fröhlich interaction between an electron and a qth confined LO-phonon mode is of the following form:[16]

$$H_{e\text{-}p}=iA_q\Phi_q(z)$$
$$=\begin{cases} iA_q\{\cos[q\pi z/(p+1)a]-(-1)^{q/2}\}, & q=\text{even} \\ iA_q\{\sin[\mu_q\pi z/(p+1)a]+C_q z/(p+1)a\}, & q=3,5,\ldots \end{cases} \tag{2}$$

where a is the width of a monolayer, pa is the well width, and μ_q and C_q are constants determined by $\tan(\mu_q\pi/2)=\mu_q\pi/2$ and $\Phi_q(z)=0$ at $z=\pm(p+1)a/2$. A_q is a normalization constant.

The Hamiltonian for a valence-band electron and the qth confined LO-phonon deformation-potential (DP) interaction is as follows:

$$H_{e\text{-}p} = iD^x_{jj'}B_q W_q(z) = \begin{cases} iD^x_{jj'}B_q \sin[q\pi z/(p+1)a], & q = \text{even} \\ iD^x_{jj'}B_q\{[\mu_q\pi/(p+1)a]\cos[\mu_q\pi z/(p+1)a] + C_q/(p+1)a\}, & q = 3,5,\ldots \end{cases} \tag{3}$$

where B_q is a normalization factor and $D^x_{jj'}$ is the DP-matrix element between the spinor components of the valence-band-edge function U_j^* and $U_{j'}$ ($j,j' = \pm\frac{3}{2}, \pm\frac{1}{2}$) for a displacement along the x direction, which are nonvanishing for displacement along the z direction when $|j-j'|=2$, and nonzero for in-plane displacement when $j'-j=\pm 1$ ($j=\frac{1}{2},\frac{3}{2}$).[18] $|D_{jj'}| = u_0 d_0/(4a)$, where u_0 is the zero-point amplitude for the optical relative displacement in the well material, which is equal to $(\hbar/2m\omega_q)^{1/2}$.

The formulas above are suitable for phonons with a nonvanishing wave vector, when the $q=1$ confined mode is developed into the so-called "interface mode."[1,15,16] But for the $z\bar{z}$ backscattering, the displacement $W_q(z)$ for the $q=1$ mode is simply proportional to $\cos[\pi z/(p+1)a]$, and for other odd modes, Eq. (3) is reformulated by removing the constant term. Of course, the Fröhlich potential in Eq. (2) for odd modes should also be reformulated for backscattering, but, as we shall show, it does not concern us due to reasons of symmetry.

We shall take the intermediate states as approximately two-subband exciton states. A two-subband exciton state derived from the μth electron subband (CBμ) and the νth heavy-hole (light-hole) HH (LH) subband (HHν or LHν) can be written in cylindrical coordinates (ρ,φ,z) as

$$|\mu,\nu,n,m\rangle = S^{-1/2}\sum_{\mathbf{k}} G_{nm}(k) f_\mu(z_e) U_0 \sum_j g^*_{\nu j}(k,0,z_h) U_j^* \exp[i(j-j_0)\theta + ik\rho\cos(\theta-\varphi)] , \tag{4}$$

where $f_\mu(z)$ is the envelope function of CBμ and U_0 is the band-edge function of the electron, and $g_{\nu j}(k,\theta,z)$ is the j spinor component of the envelope function of HHν (LHν) associated with the in-plane wave vector $\mathbf{k}=(k,\theta)$. $G(k)$ is the exciton correlation function in k space. S is the normalization area. j_0 is an index specifying the angular momentum states of the exciton introduced in Ref. 11, to be explained presently.

For a proper appreciation of the physical implications of the above exciton wave function, it is important to note the following key points about electronic structure and exciton states in MQW's.

(i) A basic feature of a hole subband in MQW's is that as in-plane wave vector $\mathbf{k}\to\mathbf{0}$, only one spinor component of the hole (to be designated as the j_d component) is nonvanishing.

(ii) Each of the four spinor components corresponds to a different in-plane angular momentum; the four successive components are characterized by angular momentum numbers successively increased by 1. Suppose j_0 were the component with zero angular momentum; then, once j_0 is known, the angular momenta of all components can be deduced. Another way of specifying the angular momentum state of an exciton is in terms of the angular momentum quantum number m associated with the j_d component of the exciton, naming the exciton as in $s,p,d,\ldots$ states according to $m=0,\pm1,\pm2,\ldots$. Here, j_0 and m are related by $j_0 = j_d - m$.

(iii) The four hole components of the exciton wave functions are alternatively even and odd with respect to z inversion.

The excitonic optical transition matrix element can be expressed as

$$\langle\mu,\nu,n,m|\mathbf{P}\cdot\hat{\boldsymbol{\varepsilon}}|0\rangle = \sqrt{S}/(2\pi)\int dk\, kG(k)\int dz\, f_\mu(z) g_{\nu j_0}(k,0,z)\langle U_0|\hat{\boldsymbol{\varepsilon}}\cdot\mathbf{P}|U_{j_0}\rangle . \tag{5}$$

The Fröhlich interaction matrix element between two exciton states coupled to the qth LO mode reads

$$\langle\mu',\nu',n',m'|H_{e\text{-}p}|\mu,\nu,n,m\rangle = iA_q S/2\pi\delta_{j_0,j_0'}\left[\delta_{\nu\nu'}\int k\,dk\, G_{n'm'}(k)G_{nm}(k)\int dz\, f^*_{\mu'}(z) f_\mu(z)\Phi_q(z) - \delta_{\mu\mu'}\int k\,dk\, G_{n'm'}(k)G_{nm}(k)\sum_{j,j'}\delta_{jj'}\int dz\, g_{\nu'j'}(k,0,z) g^*_{\nu j}(k,0,z)\Phi_q(z)\right] . \tag{6}$$

The DP interaction matrix element between two exciton states coupled to the qth LO mode with z-direction displacement is

$$\langle\mu',\nu',n',m'|H_{e\text{-}p}|\mu,\nu,n,m\rangle = -iSB_q\delta_{\mu\mu'}\int k\,dk\,\delta_{j_0,j_0'\pm2}\sum_{j,j'}\delta_{j,j'\pm2}G_{n'm'}(k)G_{nm}(k) \times\int dz\, g_{\nu'j'}(k,0,z) g^*_{\nu j}(k,0,z) W_q(z) D^z_{jj'} . \tag{7}$$

Formulas (5)–(7) provide the basis for constructing the Raman tensor, and the closely related aspects listed below are basic to a theoretical analysis of the Raman scattering.

(i) In contrast to bulk materials, in MQW's the Fröhlich mechanism of scattering is "allowed," even in the dipole approximation; in fact, realizable in two ways. On the one hand, Fröhlich interaction can lead to intersubband scattering, which finds no parallel in bulk materials. On the other hand, intrasubband electron and hole scattering do not completely cancel as in bulk materials, since the penetration into the potential barrier for the electron and for the hole is different, and the HH and LH mixing makes the density distribution of holes different from that of electrons.

(ii) Equation (5) indicates that only the j_0 component of the excitons contributes to the optical transition. From the point of view of the oscillator strength of the excitonic transition, the s-state excitons should be the most important in Raman scattering.

(iii) Equation (6) indicates that in Fröhlich scattering the j_0 value is conserved, which implies that all four components of the two intermediate excitons have completely matched orbital angular momenta. Thus, for example, the s-state HH exciton cannot be scattered into an s-state LH exciton (as they have different j_d values), even with the HH and LH mixing taken into account.

(iv) The delta symbol $\delta_{j_0,j_0'\pm 2}$ in Eq. (7) implies that DP scattering is only operative between excitons with their angular momentum components relatively shifted by two places. Thus Raman scattering due to intrasubband DP scattering must be weak (as in this case, j_d will be the same and j_0 different; therefore not both excitons can be s excitons).

(v) Formula (5) shows that for the optical transition matrix elements not to vanish, the parity of the electron wave function and the j_0 hole component with respect to z inversion must be equal, in both intermediate excitons. As the scattering between them (single-particle interaction) always leaves at least one of the electron-hole pair in its original subband, and, hence, with unchanged parity, it follows that the parity of the electron in the case of electron scattering or parity of the j_0 hole component in the case of hole scattering must also remain unchanged. Moreover, for the case of hole scattering, this implies that all four components have matched parities before and after the scattering, both for Fröhlich and DP scattering (as a shift of j by 2 does not change the parities of the four components). This means that the $\Phi_q(z)$ for Fröhlich scattering and the $W_q(z)$ for DP scattering must be even functions of z; thus $B2$ phonons are Raman active for DP scattering and $A1$ modes for Fröhlich scattering.

(vi) Since j_0 and U_{j_0} are conserved in the Fröhlich process, it is only possible for a $++$ or $--$ polarization configuration in $z\bar{z}$ backscattering; since $\Delta j_0=2$ for DP scattering, and the band-edge function changes from $X+iY$ (or $X-iY$) to $X-iY$ (or $X+iY$), it is then only possible for a $+-$ or $-+$ polarization configuration in $z\bar{z}$ backscattering. Thus, $A1$ phonons are dipole allowed for a polarized configuration and $B2$ phonons for a depolarized configuration.

As an example, we calculated the resonant Raman profile for $(GaAs)_{50\ Å}(AlAs)_{150\ Å}$, $(GaAs)_{102\ Å}$-$(Al_{0.27}Ga_{0.73}As)_{207\ Å}$, and $(GaAs)_{150\ Å}(AlAs)_{150\ Å}$. The intermediate exciton states are calculated by using the variational method of Ref. 10. The parameters used in our calculation are as follows: the DP constant $d_0=35$ eV, $P^2/m_0=12.9$ eV, and the band offset is taken to be 40:60.

In Table I, we compare the relative contributions from ten relatively dominant Fröhlich scattering channels with the $q=2$ phonon mode, for MQW's with three different well widths. The tabulated values are the calculated values for the numerator in the Raman tensor given in Eq. (1), where we have used the notation $\mu\nu H(L)nm$ to represent the CBμ-HH(LH)ν nm exciton state.

As discussed particularly in Refs. 10 and 11, the allowed ($\Delta n=0$) $1s$ exciton states usually have larger oscillator strengths, especially in narrower wells. Therefore, cases with both intermediate excitons being allowed $1s$-state excitons are expected to make important contributions to the scattering. This trend is observable in Table I. However, there are other complicating factors; thus the difference between the mutually cancelling electron and hole intrasubband Fröhlich scattering is larger in the

TABLE I. Top ten Fröhlich scattering channels (via the $A1$ phonon mode) for three samples with different well widths. The left column for each sample labels two intermediate states and the right column represents the numerators of Eq. (1) (arb. units).

50-Å well width		102-Å well width		150-Å well width	
$21L2p$	−251.3	$21L2p$	−169.6	$21L2p$	−188.6
$33H1s$	−216.1	$11H1s$-$13H1s$	138.6	$13H1s$-$33H1s$	−99.8
$11H1s$	−191.9	$11H1s$	−118.9	$33H1s$-$35H1s$	93.9
$11H1s$-$13H1s$	175.2	$33H1s$	−96.5	$11H1s$-$13H1s$	84.4
$22H1s$	−129.7	$22H1s$	−90.4	$21L2p$-$22H1s$	55.2
$13H1s$-$33H1s$	−51.1	$22H1s$-$24H1S$	64.8	$22H1s$	−45.3
$21L2p$-$22H1s$	36.4	$21L2p$-$24H1s$	39.8	$11H1s$	−41.6
$13H1s$	35.9	$13H1s$	39.8	$33H1s$	−35.9
$11L1s$	32.0	$13H1S$-$33H1S$	−37.9	$11H1s$-$31H1s$	33.3
$11H1s$-$31H1s$	31.4	$21L2P$-$22H1S$	33.3	$31H1s$-$33H1s$	−29.3

case of forbidden ($\Delta n \neq 0$) intrasubband scattering. This can become important if the forbidden exciton transition becomes moderately strong, which ultimately depends on the HH and LH mixing. Thus, the allowed intrasubband $1s$ channel dominates for narrower wells, while intersubband (no electron and hole mutual cancelling effect) and forbidden (but parity-allowed) intrasubband channels dominate in wider wells. The numerical results in the table support such considerations. The strong mixing of the HH2 into the LH1 wave function makes the $21L2p$ (CB2-LH1 $2p$-state) intrasubband channel become the most efficient channel (for the first $A1$ phonon mode) in spite of the well widths. As for DP scattering, the numerical results show that the overwhelming process is $11H1s$-$11L1s$ scattering (for the first $B2$ phonon mode) regardless of the well widths. The dependence of the scattering on the phonon modes for the 50 Å-wide sample is depicted in Table II.

In Fig. 1, we plot the calculated resonant Raman profile in the 102-Å-wide sample in the configuration $z(xx)\bar{z}$ associated with the first $A1$ phonon mode. Compared with the experiments by Zucker *et al.*,[2] the agreement is reasonably good, though only the $1s, 2s, 3s, 2p\pm, 3d$ states of excitons of all confined subbands are included in the calculation.[19] In calculating the resonant profile we have used a damping factor to simulate inhomogeneity effects corresponding to one-monolayer fluctuation.

One interesting point in the resonant profile is the asymmetry between incoming and outgoing resonances which Zucker *et al.* has attributed to intersubband exciton–LO-phonon scattering.[2,20] According to Zucker's model, outgoing resonance dominates for transition to a higher-energy state, and the incoming resonance peak is higher than the outgoing resonance peak in the case of transition to a lower-energy state. However, their argument is not adequate, because the intrasubband and intersubband scattering will create interference. As an example, let us look at the resonant peaks related to $33H1s$ in Fig. 1. The two main scattering channels are intersubband $13H1s$-$33H1s$ and intrasubband $33H1s$ (cf. Table I). If the resonant profile can be interpreted in terms of the simplified two-level system ($E_1 = 33H1s$, $E_2 = 13H1s$, $E_1 - E_2 > \hbar\omega_q$), as Zucker *et al.* did, we have the following expression:

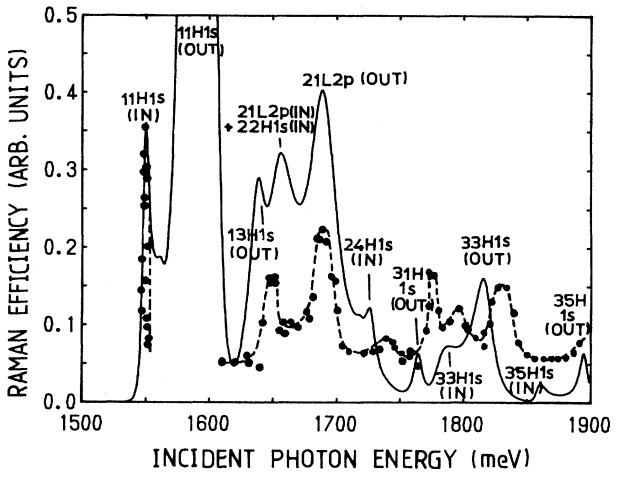

FIG. 1. Calculated squared xx component of the Raman tensor for the 102-Å-wide MQW associated with the 1st $A1$ mode vs the incident energies (solid line), compared with the experimental data of Ref. 2 (points and dashed line).

$$\left| \frac{-96.5}{(E_1-E)(E_1-E+\hbar\omega_q)} + \frac{-37.9}{(E_1-E)(E_2-E+\hbar\omega_q)} + \frac{-37.9}{(E_1+\hbar\omega_q-E)(E_2-E)} \right|^2 . \tag{8}$$

In incoming resonance ($E = E_1$), the first two terms are canceled partly; however, the first and third terms are strengthened in outgoing resonance ($E = E_1 + \hbar\omega_q$). Thus, the outgoing resonance might dominate for transitions to lower-energy states, which is contrary to Zucker's argument.

In conclusion, we have shown the Raman scattering mediated by exciton states in MQW's to depend closely

TABLE II. The dependence of the most important scattering channels on the phonon modes for the 50-Å-wide MQW's.

1st $B2$ mode		2nd $B2$ mode		3rd $B2$ mode	
$11H1s$-$11L1s$	−314.9	$22H1s$-$22L1s$	83.4	$11L1s$-$13H1s$	6.0
$22H1s$-$22L1s$	−80.3	$11L1s$-$13H1s$	62.6	$11H1s$-$11L1s$	3.9
$21L2p$-$22L1s$	−26.3	$21L2p$-$23H2p$	35.1	$21L2p$-$23H2p$	3.2
$11H2s$-$11L1s$	22.4	$11H1s$-$11L1s$	−34.9	$22H1s$-$22L1s$	3.1
1st $A1$ mode		2nd $A1$ mode		3rd $A1$ mode	
$21L2p$	−251.3	$33H1s$	108.4	$33H1s$	−113.2
$33H1s$	−216.1	$22H1s$	71.8	$22H1s$	−17.0
$11H1s$	−191.9	$11H1s$-$13H1s$	59.8	$21L2p$	−9.8
$11H1s$-$13H1s$	175.2	$21L2p$-$22H1s$	18.4	$33H2s$	−9.5

on the special characteristics of quasi-two-dimensional exciton-phonon and exciton-photon interactions. For polarized Fröhlich scattering, intrasubband exciton–A 1-phonon channels dominate for thinner wells, while intersubband exciton–A 1-phonon channels become more important for wider wells. For depolarized DP scattering, the only significant channels are the HH-exciton–B 2-phonon–LH-exciton. The combined action of the intersubband and intrasubband exciton-phonon scattering leads to the asymmetry of the incoming and outgoing resonance in the high-quality samples.

This work was supported by the China National Natural Science Foundation.

[1]A. K. Sood, J. Menéndez, M. Cardona, and K. Ploog, Phys. Rev. Lett. **54**, 2111 (1985); **54**, 2115 (1985).
[2]E. Zucker, A. Pinczuk, D. S. Chemla, A. C. Gossard, and W. Wiegmann, Phys. Rev. Lett. **51**, 1293 (1983); **53**, 1280 (1984).
[3]D. A. Kleinman, R. C. Miller, and A. C. Gossard, Phys. Rev. B **35**, 664 (1987).
[4]M. V. Klein, IEEE J. Quantum Electron. **QE-22**, 1760 (1986).
[5]A. Alexadrou, M. Cardona, and K. Ploog, Phys. Rev. B **38**, 2196 (1988).
[6]Z. P. Wang, D. S. Jiang, and K. Ploog, Solid State Commun. **65**, 661 (1987).
[7]Y. C. Chang and J. N. Shulman, Phys. Rev. B **29**, 1807 (1984); Appl. Phys. Lett. **43**, 536 (1983).
[8]K. Huang, J. B. Xia, B. F. Zhu, and H. Tang, J. Lumin. **40&41**, 88 (1988).
[9]L. J.Sham, Superlatt. Microstruct. (to be published).
[10]Bangfen Zu and Kun Huang, Phys. Rev. B **36**, 8102 (1987).
[11]Bangfen Zhu, Phys. Rev. B **37**, 4689 (1988); **38**, 13 316 (1988).
[12]G. E. W. Bauer and T. Ando, Phys. Rev. B **38**, 13 316 (1988).
[13]E. Richter and D. Strauch, Solid State Commun. **64**, 864 (1987).
[14]Shanf-Fen Ren, Hanyou Chu, and Y. C. Chang, Phys. Rev. Lett. **59**, 1841 (1987).
[15]Kun Huang and Bangfen Zhu, Phys. Rev. B **38**, 2183 (1988); Bangfen Zhu, Phys. Rev. B **38**, 7694 (1988).
[16]Kun Huang and Bangfen Zhu, Phys. Rev. B **38**, 13 377 (1988).
[17]R. M. Martin, Phys. Rev. B **4**, 3676 (1971).
[18]G. L. Bir and G. E. Pikus, Fiz. Tverd. Tela (Leningrad) **2**, 2287 (1960) [Sov. Phys.—Solid State **2**, 2039 (1961)].
[19]For the case where intermediate states are the continuous electron-hole pair, a similar theory has also been derived, which will be published elsewhere.
[20]J. E. Zucker, A. Pinczuk, and D. S. Chemla, Phys. Rev. B **38**, 4287 (1988).